Elsevier Editorial System(tm) for Quaternary Geochronology
Manuscript Draft

Manuscript Number: QUAGEO-D-10-00044R1

Title: 40Ar/39Ar geochronology of Holocene basalts; examples from Stromboli, Italy.

Article Type: Research Paper

Keywords: Stromboli, 40Ar/39Ar geochronology, volcanology, Holocene volcanism

Corresponding Author: Prof. Dr. Jan R. Wijbrans, PhD

Corresponding Author's Institution: Faculty of Earth and Life Sciences - VU University

First Author: Jan R. Wijbrans, PhD

Order of Authors: Jan R. Wijbrans, PhD; Björn Schneider; Klaudia F Kuiper, dr.; Sonia Calvari; Stefano Branca; Emanuela de Beni; Gianluca Norini; Rosa Anna Corsaro; Lucia Miraglia

Abstract: Absolute chronologies of active volcanoes and consequently timescales for eruptive behaviour and magma production form a quantitative basis for understanding the risk of volcanoes. Surprisingly, the youngest records in the geological timescale often prove to be the most elusive when it comes to isotopic dating. Absolute Holocene volcanic records almost exclusively rely on 14C ages measured on fossil wood or other forms of biogenic carbon. However, on volcanic flanks, fossil carbon is often not preserved, and of uncertain origin when present in paleosols. Also, low 14C-volcanic CO2 may have mixed with atmospheric and soil 14C-CO2, potentially causing biased ages. Even when reliable data are available, it is important to have independent corroboration of inferred chronologies as can be obtained in principle using the 40K/40Ar decay system. Here we present results of a 40Ar/39Ar dating study of basaltic groundmass in the products from the Pleistocene - Holocene boundary until the beginning of the historic era for the north-northeastern flank of Stromboli, Aeolian Islands, Italy, identifying a short phase of intensified flank effusive activity 7500±500 yrs ago, and a maximum age of 4000±900 yr for the last flank collapse event that might have caused the formation of the Sciara del Fuoco depression. We expect that under optimum conditions 40Ar/39Ar dating of basaltic groundmass samples can be used more widely for dating Holocene volcanic events.

$^{40}Ar/^{39}Ar$ geochronology of Holocene basalts; examples from Stromboli, Italy.

Jan Wijbrans[1], Björn Schneider[1], Klaudia Kuiper[1], Sonia Calvari[2], Stefano Branca[2], Emanuela De Beni[2], Gianluca Norini[3] , Rosa Anna Corsaro[2] & Lucia Miraglia[2].

[1]*Department of Earth Sciences, Faculty of Earth and Life Sciences, VU University, Amsterdam, The Netherlands*

[2]*Istituto Nazionale di Geofisica e Vulcanologia, Sezione di Catania, Catania, Italy*

[3]*Computational Geodynamics Laboratory, Centro de Geociencias, Universidad Nacional Autónoma de México, Querétaro, Mexico*

Abstract

Absolute chronologies of active volcanoes and consequently timescales for eruptive behaviour and magma production form a quantitative basis for understanding the risk of volcanoes. Surprisingly, the youngest records in the geological timescale often prove to be the most elusive when it comes to isotopic dating. Absolute Holocene volcanic records almost exclusively rely on ^{14}C ages measured on fossil wood or other forms of biogenic carbon. However, on volcanic flanks, fossil carbon is often not preserved, and of uncertain origin when present in paleosols. Also, low ^{14}C-volcanic CO_2 may have mixed with atmospheric and soil ^{14}C-CO_2, potentially causing biased ages. Even when reliable data are available, it is important to have independent corroboration of inferred chronologies as can be obtained in principle using the $^{40}K/^{40}Ar$ decay system. Here we present results of a $^{40}Ar/^{39}Ar$ dating study of basaltic groundmass in the products from the Pleistocene – Holocene boundary until the beginning of the historic era for the north-northeastern flank of Stromboli, Aeolian Islands, Italy, identifying a short phase of intensified flank effusive activity 7500±500 yrs ago, and a maximum age of 4000±900 yr for the last flank collapse event that might have caused the formation of the Sciara del Fuoco depression. We expect that under optimum conditions $^{40}Ar/^{39}Ar$ dating of basaltic groundmass samples can be used more widely for dating Holocene volcanic events.

Introduction

Definitive isotopic dating of Holocene volcanic strata often proves elusive, as such chronologies must be measured by ^{14}C on sparsely preserved fossil carbon or by the $^{40}Ar/^{39}Ar$ technique on sanidine which may contain up to 16% K_2O (*e.g.* Renne et al, 1997). $^{40}Ar/^{39}Ar$ dating of Holocene basalts that commonly contain much less K_2O when compared with sanidine is difficult because of the extremely low enrichments in radiogenic ^{40}Ar, fundamentally limiting the range of the method (Bacon and Lanphere, 2006, Renne et al., 1997, Hora et al. 2007, Singer et al., 2008, Carracedo et al., 2007, Gillot and Keller, 1993, Hora et al., 2007, Singer et al., 2008). We have applied a $^{40}Ar/^{39}Ar$ laser incremental heating technique to groundmass separates from high K-calcalkaline basalts to shoshonitic basalts (K_2O contents in the range 1.8 – 5.0%) from the lower northeast flank of Stromboli volcano and obtained plateau ages that consist in most cases of at least 6 steps and more than 95% of the total gas release. To precisely measure the radiogenic ^{40}Ar content of young basalts we have optimized signal intensities by applying sample pans that allow even heating of >100 mg basalt groundmass and we use a new laser beam delivery system that allows more even heating of the sample. In addition, for discrimination, we use correction a

^{38}Ar spiked air argon pipette system where the ^{40}Ar/^{38}Ar ratio is *ca* 2, which allows us to monitor variations in discrimination more precisely than it is possible with conventional air pipette systems (a more detailed account of our discrimination determination protocol is given in the appendix/electronic supplement). With our laser step heating technique we can achieve extremely small blanks, with blank proportions on the most important ^{40}Ar and ^{36}Ar beams commonly in the 0.1 permille range.

Stromboli's volcanic history (Hornig-Kjarsgaard et al., 1993, Keller et al., 1993, Pasquaré et al., 1993, Tanner and Calvari, 2004) consists of several cycles of topography build-up and collapse over the last *ca* 100 ka: short periods of rapid topography build-up were documented at 62±1 ka and 40±2 ka during the Paleostromboli phase (Quidelleur et al., 2005, Cortés et al. 2005), resulting in collapse of the volcano at *ca* 35 ka (Gillot and Keller, 1993). The subsequent Vancori phase was dated at 26.2±3.2 ka for the lower, 21.0±6.0 ka for the middle, and 13.0 ± 1.9 ka for the upper Vancori phase (Gillot and Keller, 1993, Hornig-Kjarsgaard et al., 1993, Quidelleur et al., 2005). The youngest activity was recorded during the *ca* 13 - 6 ka Neostromboli, and <6 ka Recent Stromboli phases (Gillot and Keller, 1993). Previous dating studies on Stromboli were carried out with the K/Ar technique. We have demonstrated in a previous study on the volcanic stratigraphy of Etna that no systematic bias can be observed between our ^{40}Ar/^{39}Ar laser incremental heating technique and K/Ar technique when applied to groundmass of basaltic rocks (Gillot and Keller, 1993; Cortés et al., 2005; De Beni et al., 2005), and the same procedure has been applied to the Stromboli case in this paper.

Geological setting of the Stromboli NE sector

Recent geological investigation performed by our group (Calvari et al., 2010) in the lower NE flank of Stromboli allowed us to reconstruct in detail the stratigraphic setting of this sector of the volcano edifice (Fig. 1). On the whole, 11 lithostratigraphic units were recognised, belonging to the Vancori, Neostromboli and Recent Stromboli periods, and whose stratigraphic relationships are summarized here.

The Vancori period is formed by three units. The lowest is the Osservatorio unit, consisting of massive lava flows cropping out along drainage gullies (MO_1 member), and by volcaniclastic deposits (MO_2 member). This unit is partially covered by a thin pyroclastic deposits (Sentiero dei Fiorentini unit) and by the Roisa unit, that consists of welded spatter ramparts and lava flow. The San Vincenzo unit represents the earliest recognised volcanics of Neostromboli period, and is mainly formed by a large scoria cone cropping out under the village of Stromboli. The lava flow related to the San Vincenzo scoria cone is well preserved along the coast at Punta Lena (Fig. 1). The Labronzo unit consists of a lava flow succession forming the main portion of the costal cliff at Punta Frontone, fed by an E-W oriented dike (Fig. 1). At the exit of the Vallonazzo gully, the base of the coast cliff is formed by the lava flows belonging to the Spiaggia Lunga unit that are directly covered by the lava flows of the Vallonazzo unit. This clear stratigraphic relationship between the two units is also recognizable along the Vallonazzo gully at about 250 m a.s.l. The Nel Cannestrà unit consists of spatter ramparts and a lava flow that partially covers the Osservatorio unit and the San Vincenzo scoria cone (Fig. 1). The Serro Adorno unit comprises spatter ramparts and a lava flow that covers with an angular unconformity the lava succession of the Labronzo unit. The Piscità unit is made up of a scoria cone and by a massive lava flow that is mostly buried by lava flows of the San Bartolo unit belonging to the Recent Stromboli period. The San Bartolo unit represents the most recent volcanic products of the study area, dated at ~4-2 ka by Arrighi et al. (2004), or between BCE 360 to CE 7 by Speranza et al. (2008). This lava flow field overlays the Roisa, Vallonazzo, Piscità and Nel Cannestrà units, filling a paleo-drainage gully carved between the Roisa and the Nel Cannestrà lava flows.

Analytical methods

All experiments were carried out on groundmass separates using our CW-laser heating system based on a Synrad 48-5 CO_2 laser, custom beam delivery system (including a Raylease scanhead under analogue control and Umicore beam expander, shutter and pointer laser) for laser single fusion and incremental heating. Samples with purified in an in-house designed sample clean up line and an MAP215-50 noble gas mass spectrometer fitted with a Balzers SEV217 SEM detector operated in current mode (gains switchable under software control between 10^7, 10^8 and 10^9 Ohm amplifier resistors, and all 5 Ar -isotopes, m/e: 36, 37, 38, 39, and 40, and their baselines at m/e: (n - 0.5) measured on the SEM detector). We optimized the conditions for mass spectrometric measurement by using sample pans that allow *ca* 100 – 200 mg of basaltic groundmass to be spread out evenly forming a layer of less than 5 grains (250 – 500 μm size range) thickness, thus allowing uniform and even heating of the entire sample (e.g. O'Connor et al., 2007). By increasing sample size we were able to achieve higher beam intensities in our mass spectrometer, and thus we can measure beam intensity ratios more precisely. Defocusing of a TEM_{00} laser beam profile will still result in Gaussian beam energy distributions and uneven heating of the sample. We have overcome this by fitting our 50W CW CO_2 laser with a beam delivery system based on an industrial scanhead that allows the application of a 200 Hz (maximum) frequency triangular current with a variable amplitude (in these experiments effectively +1.5 mm – -1.5 mm), which results in a rectangular beam pattern of 3 mm in the y-direction by 0.3 mm wide. This diffused laser beam pattern, in combination with a rastering routine of 15 1-mm spaced parallel lines applied by moving the sample pan on a motorized x-y optical stage, ensures an improved homogeneity in laser power delivered to the sample.

It is commonly observed when dating basaltic groundmass by the $^{40}Ar/^{39}Ar$ incremental heating technique that phenocryst and xenocryst phases of plagioclase, olivine or clino-pyroxene contain inherited argon in amounts that may interfere with the calculation of a precise eruption age (e.g. De Beni et al., 2005). In contrast, the groundmass microcrystalline phases of plagioclase and pyroxene host the potassium and hence radiogenic ^{40}Ar (De Beni et al., 2005, Koppers et al., 2000). Therefore the sample preparation procedure focused on the selection of homogeneous fragments of basalt groundmass, and to exclude any phenocryst phases. All incremental heating experiments were carried out on 100 - 200 mg splits of 250 – 500 μm groundmass separates. Experiments were loaded in 65 mm diameter Cu-heating trays each with 5 large positions: 17 mm diameter, 3 mm deep depressions with vertical walls, made out of oxygen free Cu-rod). There were two exceptions where we applied different approaches, both involved sample STR83: the first experiment on STR83 was carried out as multiple three step fusion experiments: the first step was discarded as it contained a large amount of atmospheric argon, and the second and third steps were analyzed and regressed as multiple single fusion experiments. The second experiment on STR83 was analyzed using a resistance furnace heating technique, and a newly designed semi-automated gas clean-up line and a quadrupole mass spectrometer fitted with a dual Faraday-collector – miniature Channeltron pulse counting SEM detector, described in more detail elsewhere (Schneider et al., 2009).

The laboratory technique is described in Wijbrans et al. (1995), and the age of our laboratory standard sanidine DRA of 25.26 ± 0.2 Ma was modified in accordance to recommendations of Renne et al. (1998). In this paper we have applied the decay constants and the isotopic abundance of ^{40}K as recommended by Steiger and Jäger (1977). Data is presented with 1-σ uncertainty levels. Recently, a number of laboratories reached consensus to about a new *ca* 0.7% higher value for the common K-Ar standards used in $^{40}Ar/^{39}Ar$ geochronology for monitoring the neutron flux to which the samples were exposed (Renne et al., 2009; Kuiper et al., 2008). The extremely low enrichments in radiogenic ^{40}Ar require accurate monitoring of the mass discrimination of the mass spectrometer (our technique is discussed in detail by Kuiper, 2003, and Kuiper et al., 2004). We have chosen in this paper to follow the Steiger and Jäger (1977) convention for the isotopic composition of atmospheric argon as well. Based on the measurements of Nier and co-workers in the late 1940's (Nier, 1950) it has been accepted that the $^{40}Ar/^{36}Ar$ ratio of air is 295.5 ± 0.5. Recently, the determination of the air $^{40}Ar/^{36}Ar$ was repeated with a reported result of 298.56 ± 0.31 (Lee et al., 2006). The effect of this revised value on the actual ages reported here is likely to be minor, as in principle with our technique we measure the enrichment of samples against a determination of the composition of air on one single instrument.

Laser incremental heating of basalt groundmass shows characteristic features common to all experiments (9 samples and 2 duplicate runs by groundmass incremental heating on *ca* 100 – 200 mg sample; one experiment, STR83, was analyzed with a 3 step fusion on 15 *ca* 20 mg replicate splits of the sample): all have obviously very low (<5.0%) enrichments in radiogenic ^{40}Ar, ranging from 1.1 – 4.4% in the youngest sample that was considered to yield a reliable age (STR108) and between 1.8 – 13.1% in the oldest sample (STR101). The sample having the highest K/Ca ratio (STR114) showed enrichments of 1.3 – 4.6%. Sample STR117, considered to be the youngest on both stratigraphic basis and recent archeomagnetic dating (*ca* 2 – 4 ka; Arrighi et al., 2004; Speranza et al., 2008), gave the lowest enrichment in radiogenic ^{40}Ar ranging 0.1 – 1.2 percent, consistent with its very young age. Its calculated age of 13.1 ± 4.6 ka is inconsistent with stratigraphy, and it may be affected by its very low enrichment in radiogenic ^{40}Ar. All experiments show variable K/Ca ratios, commonly high in the first half of the experiment and low in the final steps. Average K/Ca values reflect the range in chemical compositions from 0.25 (STR117) to 1.24 (STR114), reflecting the potassium enriched nature of these basalts.

Results

We have selected nine samples for $^{40}Ar/^{39}Ar$ dating from the lithostratigraphic units of the northeast flank of Stromboli volcano as defined by Calvari et al. (2010), that are also characterised from a compositional point of view (Fig. 1 and Table 1 for a summary; full analytical data tables are found in electronic supplements to this paper). The results are represented as plateau ages with uncertainties quoted at 1-σ. The lowest stratigraphic unit for which we have a dated sample is the Roisa unit. The sample is made of spatter (STR101), and gave an age of 15.2 ± 2.8 ka (Fig. 2, Table 1, and electronic supplement). The second sample comes from the San Vincenzo unit, and is a lava flow collected at Punta Lena along the shore. The sample (STR65, Fig. 2) has an age of 12.5 ± 2.6 ka. We have dated the dyke and the lava flow of the Labronzo unit obtaining ages of 8.2 ± 1.8 ka and 8.3 ± 1.6 ka respectively (STR112 and STR115b, Table 1 and Fig. 1). A lava flow from the top of the succession of the Spiaggia Lunga unit, cropping out at the exit of the Vallonazzo gully, gave an age of 7.7 ± 1.4 ka (STR110). A lava flow from the base of the Vallonazzo unit (STR72b, Table 1 and Fig. 1, Fig. 2), resting directly on the Spiaggia Lunga unit, gave an age of 8.7 ± 2.0 ka. A spatter belonging to the Nel Cannestrà unit (STR83, 450 m a.s.l.), whose lava flow partially covers the San Vincenzo scoria cone, resulted in an age of 7.9 ± 1.2 ka (Fig. 2). From the Serro Adorno unit we have sampled a lava flow (STR114, 2 m a.s.l.) for which we obtained an age of 6.9 ± 1.1 ka (Fig. 2). A lava flow sample from the Piscità unit (STR106), overlying the products of the Roisa unit and covered by the San Bartolo lava flows, resulted in an age of 6.8 ± 1.4 ka (Fig. 2). From the San Bartolo lava flow field, which is at the top of the sequence in the study area (~4-2 ka, Arrighi et al. 2004; Speranza et al., 2008), we have sampled the highest lava flow exposed along the coast. This sample (STR117, Table 1, Fig. 2) gave us an age of 13.1 ± 4.6 ka. Finally, sample STR108 (age: 4.0 ± 0.9 ka, Fig. 2) comes from the top of the lava flow succession at Semaforo Labronzo locality that is directly covered by the Secche di Lazzaro pyroclastic deposit (Bertagnini and Landi, 1996). Although located outside the study area of Calvari et al. (2010) (Fig. 1), this lava flow provides the first firm age constraint for the end of the Neostromboli period and the Sciara del Fuoco first collapse. The only previous age constraint is an archeomagnetic maximum age of CE 1350±60, obtained by high-resolution paleo-declination determination (Arrighi et al., 2004), which apparently records a more recent and localized event.

Discussion

All ages derived for this study are based on a high resolution laser incremental heating method that allows us to resolve the admixture of phenocryst-hosted inherited ^{40}Ar in the final temperature steps of the incremental heating experiments that would not be possible in more common single fusion or low-resolution furnace experiments (e.g. Hora et al., 2007; or Singer et al., 2008). As mentioned before, we are unable to detect any biases between our $^{40}Ar/^{39}Ar$ technique and K/Ar ages where we carried out experiments on rocks from the same outcrops. Our result is consistent with that of Foeken et al. (2009) who published a cosmogenic ^{3}He age of 6.8 ± 0.2 ka for samples belonging to the Neostromboli phase from the western flank of the volcano.

Our results are in general agreement with the stratigraphical order defined by Calvari et al. (2010), as illustrated by the ages for San Vincenzo (12.5±2.6 ka) and Nel Cannestrà (7.9±1.2 ka) units that show clear stratigraphic relationships. An epiclastic deposit between these two units indicates a hiatus during which significant erosion occurred. Conversely, most flows yielded ages in a narrow range of *ca* 2000 years between ~9 – 7 ka, without field evidence for significant pauses in the eruptive activity. Although in general stratigraphic order, measured ages falling in this short time interval yielded statistically overlapping results, as is illustrated for the Vallonazzo and Spiaggia Lunga units, where calculated ages appear reversed but with overlapping uncertainties with respect to their stratigraphic relationship.

When data from individual experiments are regressed in isochrons, the dispersion of points is often too little to calculate reliable regression lines. However, when all data of the Neostromboli flank eruptions are regressed, the $^{40}Ar/^{36}Ar$ intercept is 296.5 ± 0.5 (n=71), which at 95% confidence level is indistinguishable from $^{40}Ar/^{36}Ar_{air}$. We interpret this to indicate that the groundmass of the rocks erupted during the Neostromboli period was essentially free of extraneous ^{40}Ar. Therefore, we quote the weighted mean plateau ages (as defined by commonly used criteria, c.f. O'Connor et al., (2007) for a discussion) as the best representation of the eruption age of individual flows. The weighted mean age of 7500 ± 500 a derived from all the results obtained for the Neostromboli period can be interpreted conservatively as the mean age for this period of increased magmatic activity. Our data set reveals consistent results that we interpret to be the culmination of the Neostromboli phase ~7500 years ago. As enrichments in $^{40}Ar^*$ are very low, the results are sensitive to bias when minute amounts of argon from other sources are present. This is illustrated by the fact that one of the highest units in the sequence, the San Bartolo lava, yielded an apparent age of 13.1 ± 4.6 ka instead of an age of ca 6 ka as expected from stratigraphic relationships with other dated units. This result stands out in that it is much older than expected, albeit that its uncertainty at the 95% confidence level is still consistent with the total data set.

Conclusion

With this study we demonstrate that $^{40}Ar/^{39}Ar$ groundmass dating Holocene high K-calcalcaline to shoshonitic basalts of Stromboli is possible under favourable conditions, obtaining results with an uncertainty margin ranging from 15% to 23%. Our results were used by Calvari et al. (2010) to date seven newly discovered eruptive fissures in the northeast flank of Stromboli and ranging from 15 to 4 ka in age, culminating with a short period of increased flank activity as recent as 7500 ± 500 years ago. With these results we confirm that during the life time of Stromboli volcano magma production was episodic, with the locus of eruptive activity changing, especially during the Neostromboli period, from the volcano flanks to the summit crater. Periods of rapid building-up of relief lead to unstable topography that may involve future hazards, including renewed flank collapse and associated tsunami hazards. The new 4.0±0.9 ka age for the Sciara del Fuoco collapse presents a more precise, younger age bracket for this most recent major catastrophic collapse event, placing it at the beginning of the 2nd millennium BC.

Acknowledgements

The mapping of Stromboli was supported by a grant to S. Calvari (Project V2/01, 2005-2007, funded by the Istituto Nazionale di Geofisica e Vulcanologia (INGV) and by the Italian Civil Protection). The sample preparation was carried out by Roel van Elsas of the Institute of Earth Sciences, VU. The new instrumentation in the argon laboratory Institute of Earth Sciences, VU (instrument grant for the CO_2 laser, AGES extraction line) was supported by grants from the ISES, VU-Energy conservation fund and the Institute of Earth Sciences). This work was partly supported by INGV through a research grant financed by MIUR-FIRB to G.N.

References Cited

Arrighi S., Rosi M., Tanguy J.C., and Courtillot V., 2004, Recent eruptive history of Stromboli (Aeolian Islands, Italy) determined from high-accuracy archeomagnetic dating, Geophysical Research Letters v. 31. L19603, doi:10.1029/2004GL020627.

Bacon C.R., and Lanphere M.A., 2006, Eruptive history and geochronology of Mount Mazama and the Crater Lake region, Oregon. GSA Bulletin v. 118, p. 1331-1359.

Bertagnini A., and Landi P., 1996, The Secche di San Lazzaro pyroclastics of Stromboli volcano: a pheatomagmatic eruption related to the Sciara del Fuoco sector collapse. Bulletin of Volcanology v. 58, p. 239-245.

Calvari S., Branca S., Corsaro R. A., De Beni E., Miraglia L., Norini G., Wijbrans J. R. and Boschi E., 2010, Reconstruction of the eruptive activity on the NE sector of Stromboli volcano: timing of flank eruptions during the past 15 ka. In print in Bulletin of Volcanology.

Carracedo J.C., Rodríguez Badiola E., Guillou H., Paterne M., Scaillet S., Pérez Torrado F.J., Paris R., Fra-Paleo U., and Hansen A., 2007, Eruptive and structural history of Teide Volcano and rift zones of Tenerife, Canary Islands. GSA Bulletin v. 119, p. 1027-1051.

Cortés J.A., Wilson M., Condliffe E., Francalanci L., and Chertkoff D.G., 2005, The evolution of the magmatic system of Stromboli volcano during the Vancori period (26–13.8 ky). Journal of Volcanology and Geothermal Research v. 147, p. 1-38.

De Beni E., Wijbrans J. R., Branca S., Coltelli M., and Groppelli G., 2005, New results of $^{40}Ar/^{39}Ar$ dating constrain the timing of transition from fissure-type to central volcanism at Mount Etna (Italy). Terra Nova v. 17, p. 292-298.

Foeken J.P.T., Stuart F.M., and Francalanci L.,2009, Dating Holocene lavas on Stromboli, Italy using cosmogenic He. Quaternary Geochronology v. 4, p. 517–524.

Gillot P.Y., and Keller J., 1993, Radiochronological dating of Stromboli. Acta Vulcanologica v. 3, p. 69-77.

Hora J.M., Singer, B.S., and Wörner, G., 2007, Volcano evolution and eruptive flux on the thick crust of the Andean Central Volcanic Zone: $^{40}Ar/^{39}Ar$ constraints from Volcan Parinacota, Chile. GSA Bulletin v. 119, p. 343-362.

Hornig-Kjarsgaard I., Keller J., Koberski U., Stadlbauer E., Francalanci L., and Lenhart R., 1993, Geology, stratigraphy and volcanological evolution of the island of Stromboli Aeolian arc, Italy. Acta Vulcanologica v. 3, p. 21- 68.

Keller J., Horning-Kjarsgaard I., Koberski U., Stadlbauer E., and Lenhart R., 1993, Geology, stratigraphy and volcanological evolution of the island of Stromboli Aeolian arc, Italy. Acta Vulcanologica 3, appended map of Stromboli, 1:10,000.

Kuiper K. F., Hilgen F. J., Steenbrink J., Wijbrans J. R., 2004, $^{40}Ar/^{39}Ar$ ages of tephras intercalated in astronomical tuned Neogene sedimentary sequences in the Eastern Mediterranean, Earth and Planetary Science Letters v. 222, 583 - 597.

Kuiper K.F., Deino A., Hilgen F.J., Krijgsman W., Renne P.R., Wijbrans J.R., (2008), Synchronizing Rock Clocks of Earth History. Science 320, 500 – 504 (87) doi: 10.1126/science.1154339

Koppers A. A. P., Staudigel H., Wijbrans J. R., 2000, Dating crystalline groundmass separates of altered Cretaceous seamount basalts by the $^{40}Ar/^{39}Ar$ incremental heating technique. Chemical Geology **166**, 139 (2000).

Lee, J-Y., Marti, K., Severinghaus, J.P., Kawamura, K., Yoo, H-S., Lee, J.B., Kim, J.S., 2006. A redetermination of the isotopic abundances of atmospheric Ar. Geochim. Cosmochim. Acta 70, 4507-4512.

Nier, A.O., 1950. A redetermination of the relative abundances of the isotopes of carbon, nitrogen, oxygen, argon, and potassium. Phys. Rev. v. 77, 789-793.

O'Connor J. M., Stoffers P., Wijbrans J. R., and Worthington T. J., 2007, Migration of widespread long-lived volcanism across the Galápagos Volcanic Province: Evidence for a broad hotspot melting anomaly? Earth and Planetary Science Letters v. 263, p. 339-354.

Pasquaré G., Francalanci L., Garduño V. H., and Tibaldi A., 1993, Structure and geologic evo-lution of the Stromboli volcano, Aeolian Islands, Italy. Acta Vulcanologica v. 3, p. 79-89.

Quidelleur X., Gillot P.Y., Filoche G., and Lefèvre J.C., 2005, Fast geochemical changes and rapid lava accumulation Stromboli Island (Italy) inferred from K–Ar dating and paleomagnetic variations recorded at 60 and 40 ka. Journal of Volcanology and Geothermal Research v. 141, p. 177-193.

Renne P.R., Sharp W.D., Deino A.L., Orsi G., and Civetta L., 1997, $^{40}Ar/^{39}Ar$ Dating into the Historical Realm: Calibration Against Pliny the Younger. Science v. 277, p. 1279-1280.

Renne P. R, Swisher C. C., Deino A. L., Karner D. B., Owens T. L., DePaolo D. J., 1998, Intercalibration of standards, absolute ages and uncertainties in $^{40}Ar/^{39}Ar$ dating. Chemical Geology v. 145, 117 - 152.

Renne P.R., Deino A.L., Hames W.E., Heizler M.T., Hemming S.R., Hodges K.V., Koppers A.A.P., Mark D.F., D Morgan L.E., Phillips D., Singer B.S., Turrin B.D., Villa I.M., Villeneuve M. Wijbrans J.R., (2009) Data reporting norms for $^{40}Ar/^{39}Ar$ geochronology. Quaternary Geochronology 4 (2009) 346–352. doi:10.1016/j.quageo.2009.06.005

Schneider B., Kuiper K.F., Postma O., Wijbrans J. (2009) $^{40}Ar/^{39}Ar$ geochronology using a quadrupole mass spectrometer. Quaternary Geochronology. doi:10.1016/j.quageo.2009.08.003

Singer B.S., Jicha B.R., Harper M.A., Naranjo J.A., Lara L.E., Moreno-Roa H., 2008, Eruptive history, geochronology, and magmatic evolution of the Puyehue-Cordon Caulle volcanic complex, Chile. GSA Bulletin v. 120 p. 599-618.

Speranza F., Pompilio M., and Sagnotti L., 2004, Paleomagnetism of spatter lavas from Stromboli volcano (Aeolian Islands, Italy): Implications for the age of paroxysmal eruptions. Geophysical Research Letters v. 31, L02607, doi:10.1029/2003GL018944.

Speranza F., Pompilio M., D'Aiello Caracciolo F., and Sagnotti L., 2008, Holocene eruptive history of the Stromboli volcano: constraints from paleomagnetic dating. Journal of Geophysical Research v. 113, B09101. doi:10.1029/2007JB005139.

Steiger R. H., Jäger E., 1977, Subcommission on geochronology: Convention on the use ofdecay constants in geo- and cosmochronology. Earth and Planetary Science Letters v. 36, 359 – 362.

Tanner L.H., and Calvari S., 2004, Unusual sedimentary deposits on the SE side of Stromboli volcano, Italy: products of a tsunami caused by the ca. 5000 years BP Sciara del Fuoco collapse? Journal of Volcanology and Geothermal Research v. 137, 329-340.

Wijbrans J.R., Pringle M.S., Koppers A.A.P., Scheveers R., 1995, Argon geochronology of small samples using the Vulkaan argon laserprobe. Proceedings Kon. Ned. Akad. v. Wetensch. V. 98, 185-218.

Figures

Figure 1.

Schematic geological map with a DEM of NE flank of Stromboli as the basis, after Calvari et al. (2010) showing sample locations. Inset top right: Location of Stromboli in the Tyrrhenian Sea showing its position with respect to the coastline of southern Italy and Sicily. Inset bottom left: Proposed stratigraphy for the map area (Calvari et al., 2010).

Figure 2.

a. combined result replicate runs on STR108a and b. from Semaforo Labronzo. b. Age spectrum STR108 first replicate. c. Age spectrum STR108 second replicate. d. Sample STR106 from the Piscità unit; e. Sample STR114 from the Serro Adorno unit; f. sample ZSTR110 from the Spiaggia Lunga unit; g. sample STR83 from the Nel Cannestrà unit. Experiment STR83a represents the second and third steps of three step fusion experiments that consist of a first step to remove a proportion of the atmospheric argon component (these steps have not been analysed), and a second step at intermediate laser power and a third step that fused the sample (9 replicate experiments). h. Experiment STR83b was carried out on the AGES furnace system and measured on a Hiden quadrupole mass spectrometer (Schneider et al. 2009); i. combined result of STR83a+b.

j. STR115b from the Labronzo unit; k. STR112 dyke unit from Labronzo; l. sample STR72b from the Vallonazzo unit; m. sample STR65 from the San Vincenzo unit; n. sample STR117 from the San Bartolo unit; o. sample STR101 from the Roisa unit.

Tables

Table 1: Summary of $^{40}Ar/^{39}Ar$ dating and sample locations.Supplementary Information:

Electronic supplement

Summary Table 1. Data summaries consisting of table, age spectrum plot, K/Ca plot, and inverse isochron (Wijbrans-summary data.pdf).

Summary Table 2. Full data tables in Excel format

(Not provided but a ZIP archive containing Excel format workbooks is available at: **http://www.geo.vu.nl/~wijj/Stromboli_data**).

Appendix 1. Monitoring of mass discrimination with a ^{38}Ar-spiked reference gas.

Appendix 2. Isochron for pooled result of STR72b, 83, 106, 110, 112, 115b, 114, 117, representing the units belonging to the Holocene Neostromboli period.

Figure

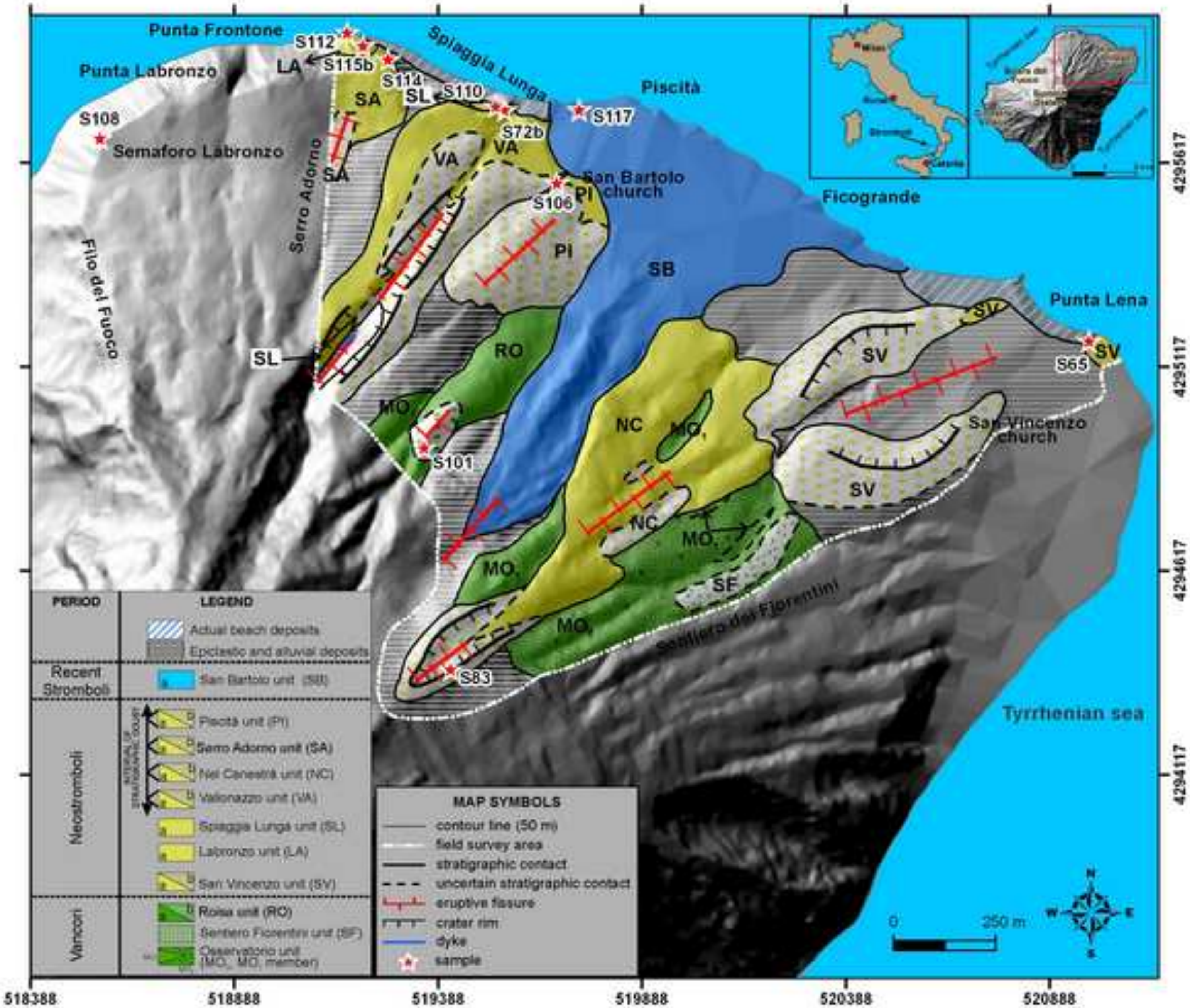
Punta Frontone
Punta Labronzo
S112
S115b
LA
S114
SL
S110
Spiaggia Lunga
S117
Piscità
S108
Semaforo Labronzo
SA
S72b
VA
Serro Adorno
San Bartolo church
S106
PI
Filo del Fuoco
SB
Ficogrande
Punta Lena
SL
RO
SV
S65
MO
S101
NC
San Vincenzo church
MO
SF
Sentiero dei Fiorentini
S83
Tyrrhenian sea
PERIOD
LEGEND
Actual beach deposits
Epiclastic and alluvial deposits
Recent Stromboli
San Bartolo unit (SB)
Neostromboli
Piscità unit (PI)
Serro Adorno unit (SA)
Nel Canestrà unit (NC)
Vallonazzo unit (VA)
Spiaggia Lunga unit (SL)
Labronzo unit (LA)
San Vincenzo unit (SV)
Vancori
Roisa unit (RO)
Sentiero Fiorentini unit (SF)
Osservatorio unit
MAP SYMBOLS
contour line (50 m)
field survey area
stratigraphic contact
uncertain stratigraphic contact
eruptive fissure
crater rim
dyke
sample
0
250 m
N
E
S
W
518388
518888
519388
519888
520388
520888
4295617
4295117
4294617
4294117

Figure

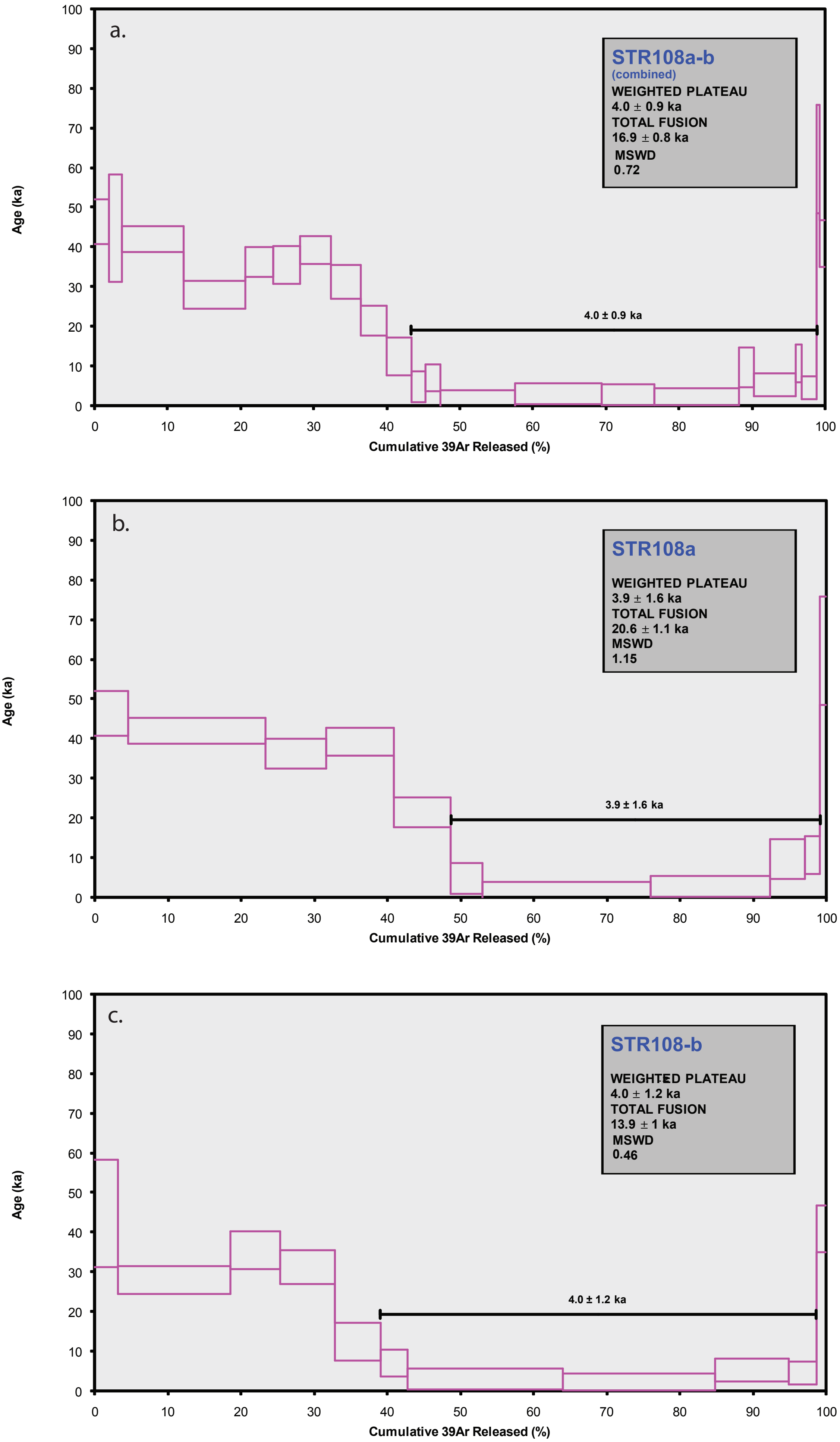
a.
STR108a-b
(combined)
WEIGHTED PLATEAU
4.0 ± 0.9 ka
TOTAL FUSION
16.9 ± 0.8 ka
MSWD
0.72
4.0 ± 0.9 ka
Age (ka)
Cumulative 39Ar Released (%)
b.
STR108a
WEIGHTED PLATEAU
3.9 ± 1.6 ka
TOTAL FUSION
20.6 ± 1.1 ka
MSWD
1.15
3.9 ± 1.6 ka
Age (ka)
Cumulative 39Ar Released (%)
c.
STR108-b
WEIGHTED PLATEAU
4.0 ± 1.2 ka
TOTAL FUSION
13.9 ± 1 ka
MSWD
0.46
4.0 ± 1.2 ka
Age (ka)
Cumulative 39Ar Released (%)

Figure

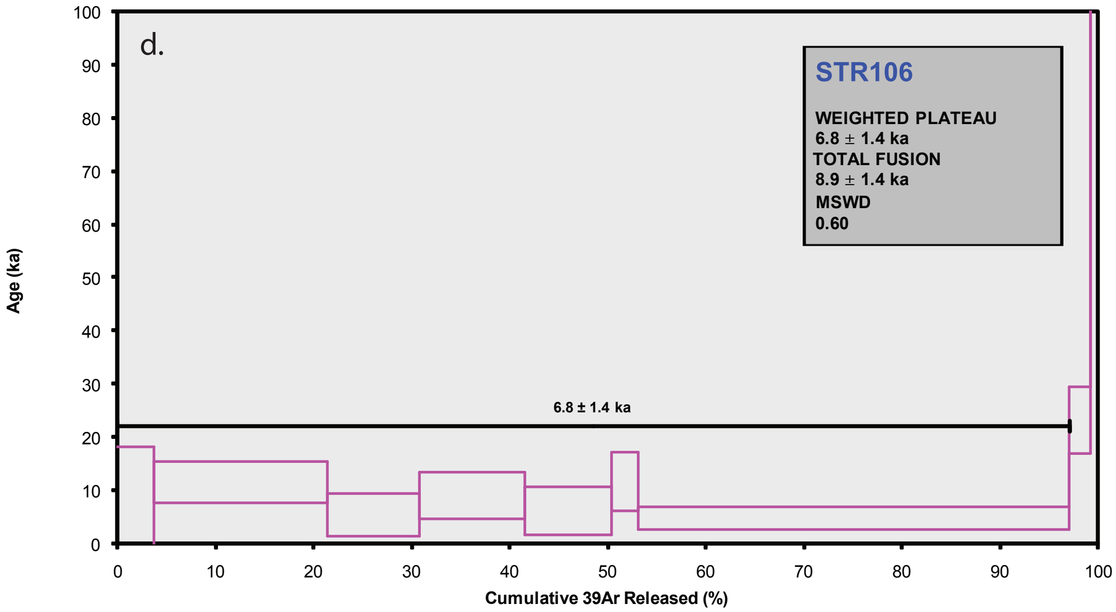
d.
STR106
WEIGHTED PLATEAU
6.8 ± 1.4 ka
TOTAL FUSION
8.9 ± 1.4 ka
MSWD
0.60
6.8 ± 1.4 ka
Age (ka)
Cumulative 39Ar Released (%)

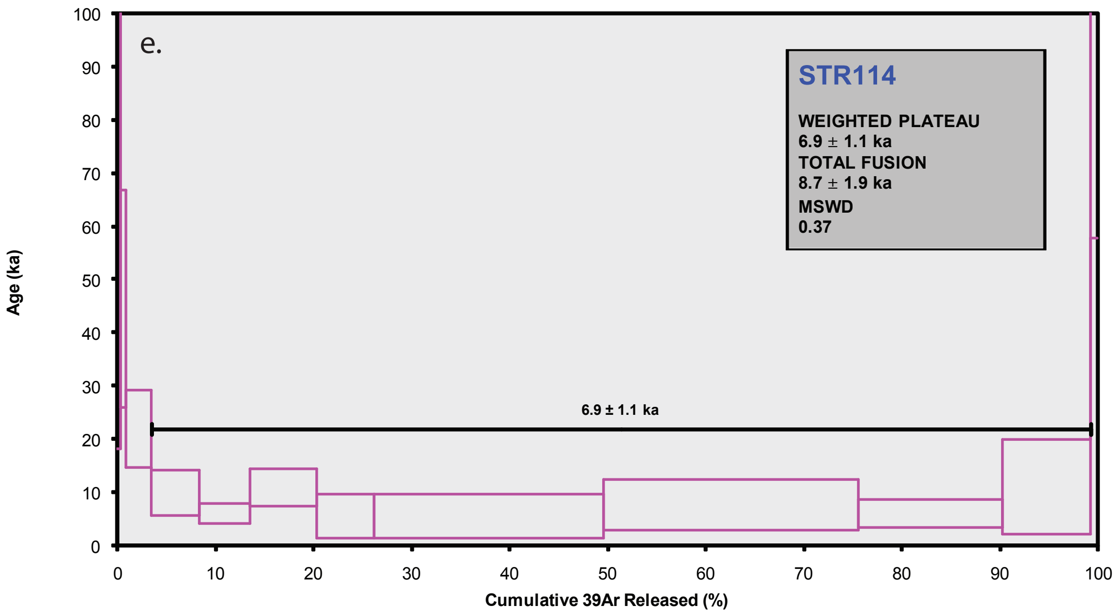
e.
STR114
WEIGHTED PLATEAU
6.9 ± 1.1 ka
TOTAL FUSION
8.7 ± 1.9 ka
MSWD
0.37
6.9 ± 1.1 ka
Age (ka)
Cumulative 39Ar Released (%)

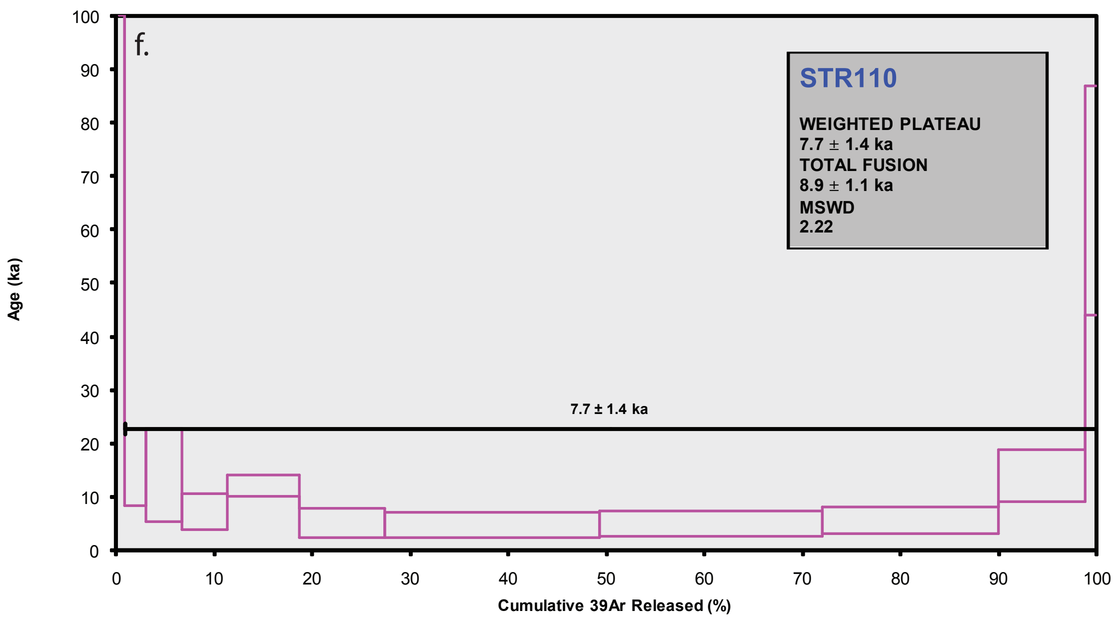
f.
STR110
WEIGHTED PLATEAU
7.7 ± 1.4 ka
TOTAL FUSION
8.9 ± 1.1 ka
MSWD
2.22
7.7 ± 1.4 ka
Age (ka)
Cumulative 39Ar Released (%)

Figure

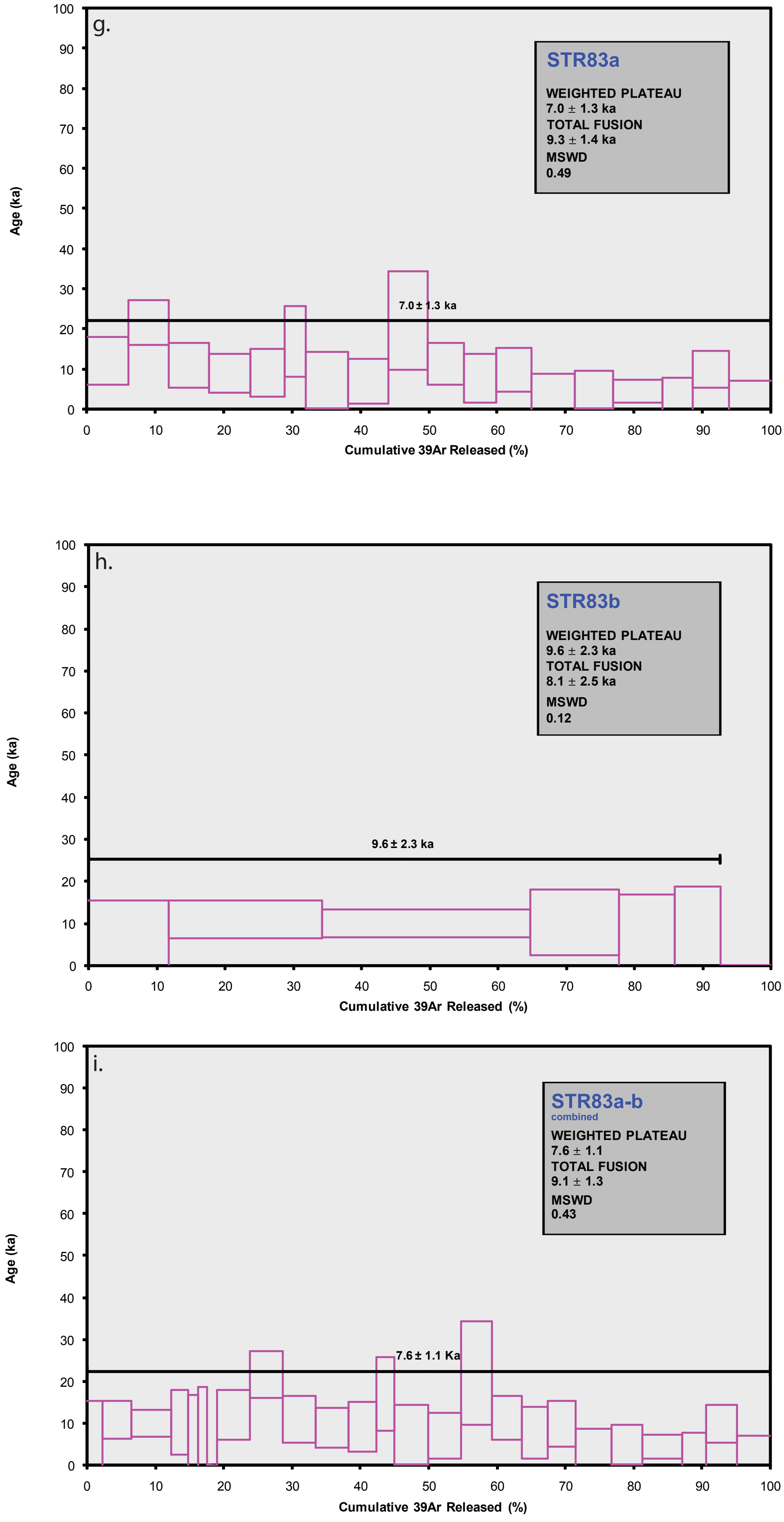
g.
STR83a
WEIGHTED PLATEAU
7.0 ± 1.3 ka
TOTAL FUSION
9.3 ± 1.4 ka
MSWD
0.49
7.0 ± 1.3 ka
Age (ka)
Cumulative 39Ar Released (%)
0
10
20
30
40
50
60
70
80
90
100
h.
STR83b
WEIGHTED PLATEAU
9.6 ± 2.3 ka
TOTAL FUSION
8.1 ± 2.5 ka
MSWD
0.12
9.6 ± 2.3 ka
Age (ka)
Cumulative 39Ar Released (%)
i.
STR83a-b
combined
WEIGHTED PLATEAU
7.6 ± 1.1
TOTAL FUSION
9.1 ± 1.3
MSWD
0.43
7.6 ± 1.1 Ka
Age (ka)
Cumulative 39Ar Released (%)

Figure

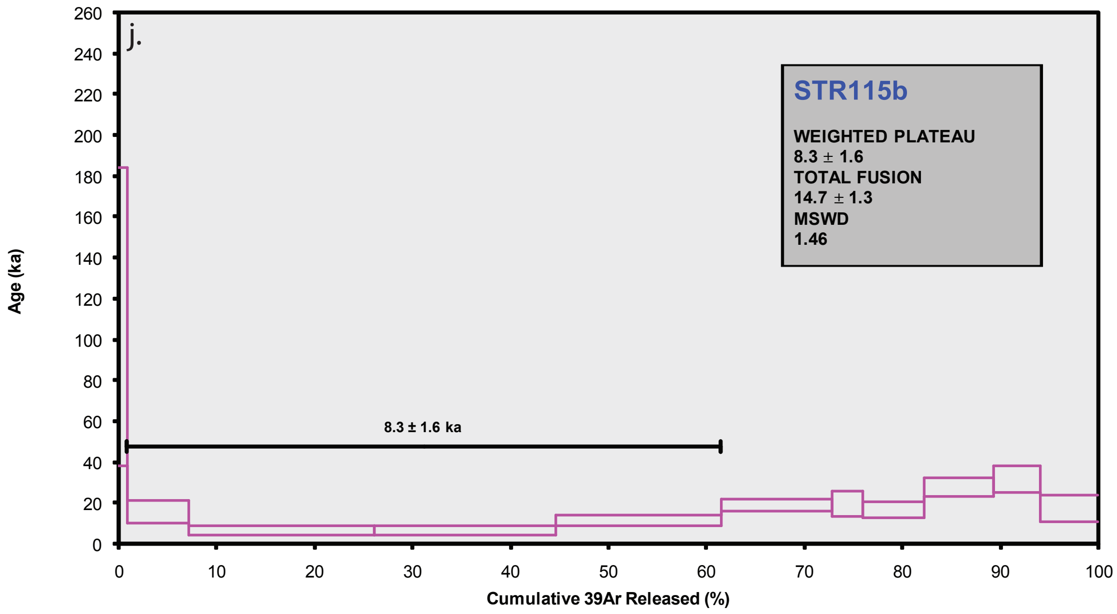
j.
STR115b
WEIGHTED PLATEAU
8.3 ± 1.6
TOTAL FUSION
14.7 ± 1.3
MSWD
1.46
8.3 ± 1.6 ka
Age (ka)
Cumulative 39Ar Released (%)

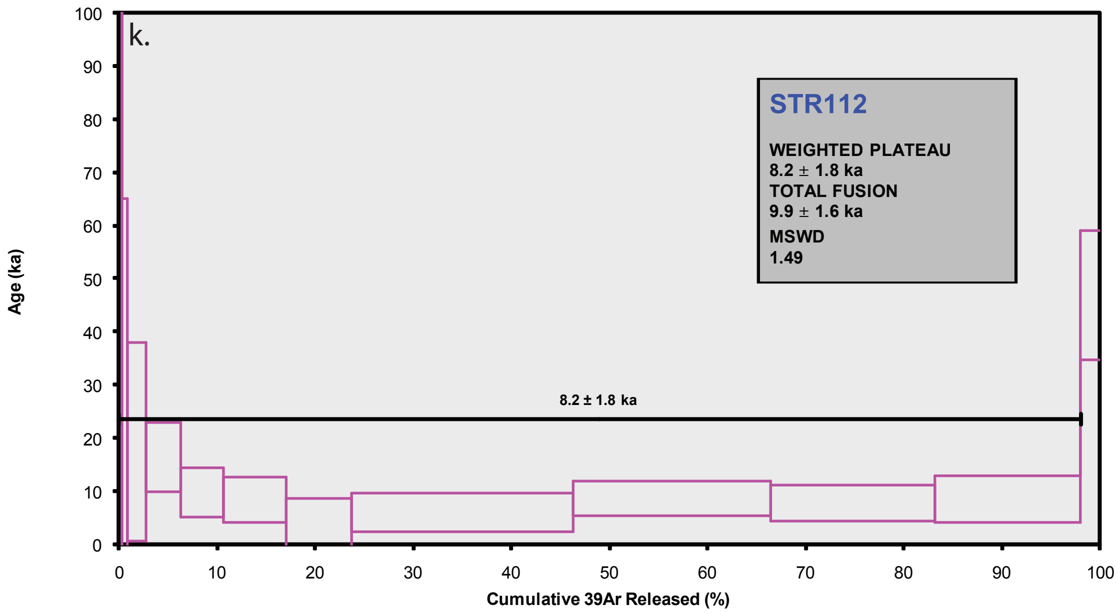
k.
STR112
WEIGHTED PLATEAU
8.2 ± 1.8 ka
TOTAL FUSION
9.9 ± 1.6 ka
MSWD
1.49
8.2 ± 1.8 ka
Age (ka)
Cumulative 39Ar Released (%)

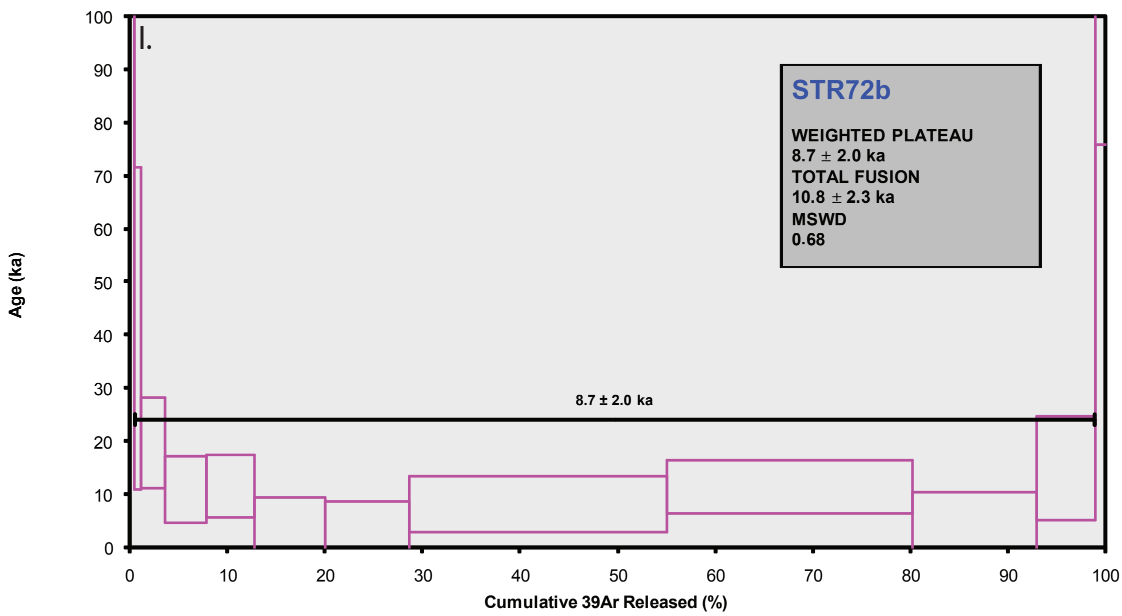
l.
STR72b
WEIGHTED PLATEAU
8.7 ± 2.0 ka
TOTAL FUSION
10.8 ± 2.3 ka
MSWD
0.68
8.7 ± 2.0 ka
Age (ka)
Cumulative 39Ar Released (%)

Figure

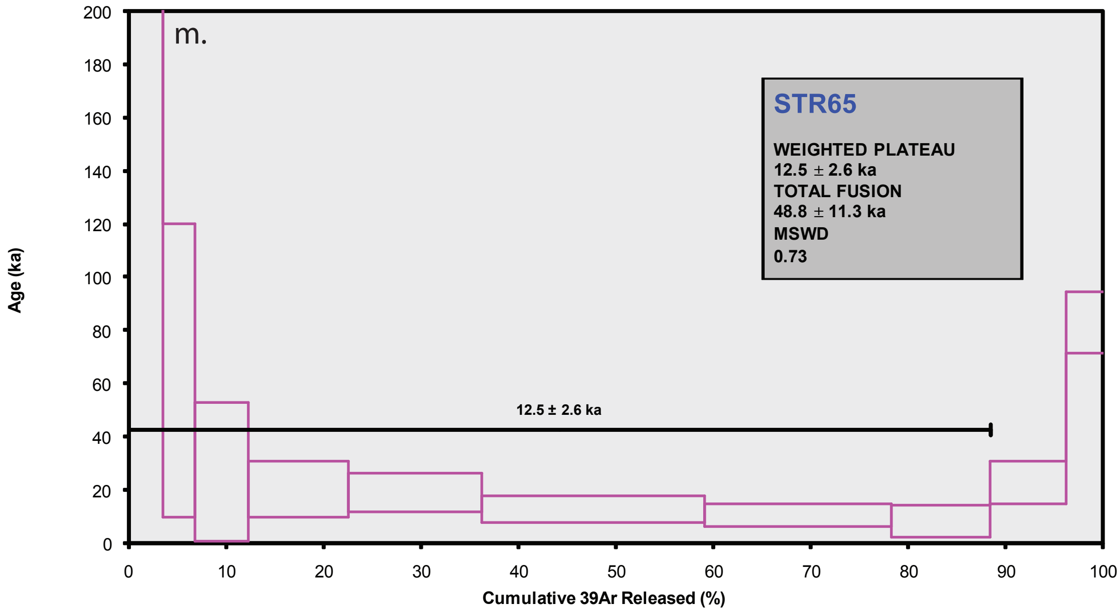
m.
STR65
WEIGHTED PLATEAU
12.5 ± 2.6 ka
TOTAL FUSION
48.8 ± 11.3 ka
MSWD
0.73
12.5 ± 2.6 ka
Age (ka)
Cumulative 39Ar Released (%)

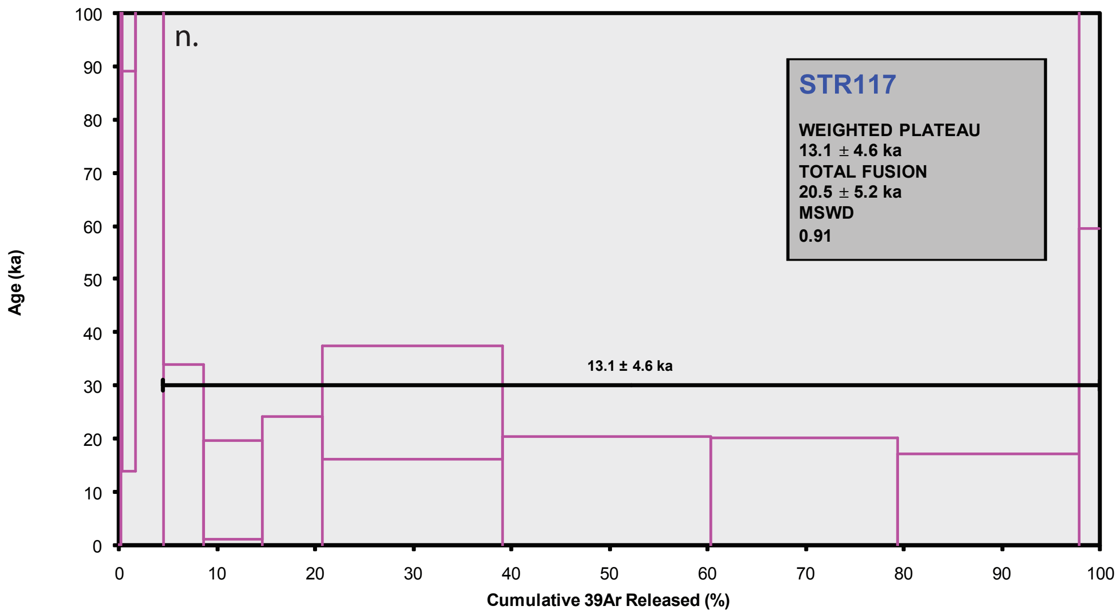
n.
STR117
WEIGHTED PLATEAU
13.1 ± 4.6 ka
TOTAL FUSION
20.5 ± 5.2 ka
MSWD
0.91
13.1 ± 4.6 ka
Age (ka)
Cumulative 39Ar Released (%)

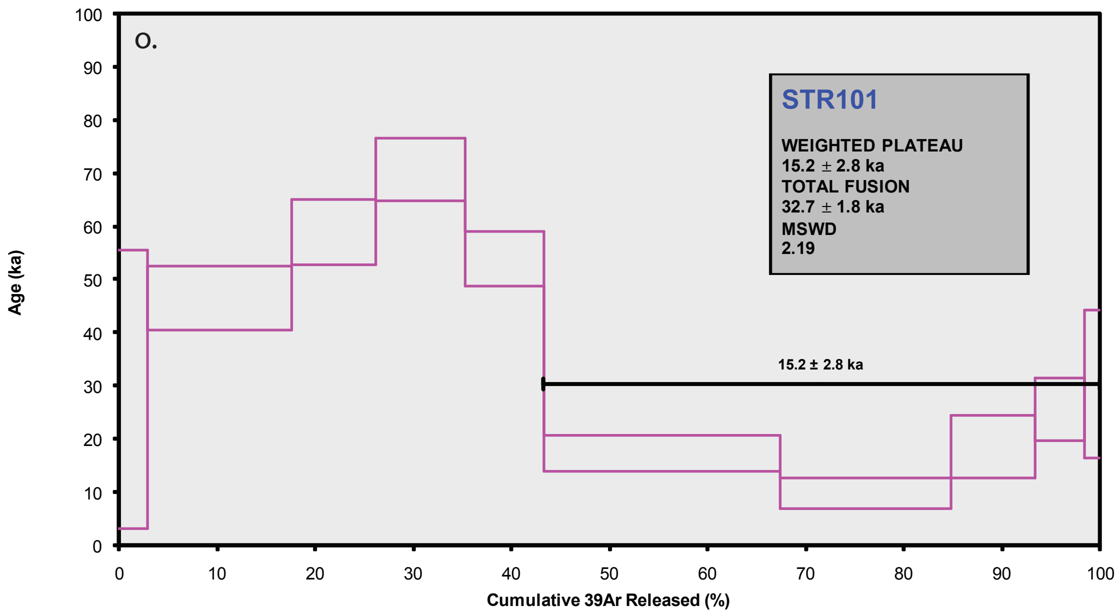
o.
STR101
WEIGHTED PLATEAU
15.2 ± 2.8 ka
TOTAL FUSION
32.7 ± 1.8 ka
MSWD
2.19
15.2 ± 2.8 ka
Age (ka)
Cumulative 39Ar Released (%)

Table

sample	litostratigraphic unit	Coordinate UTM WGS 84	Elevation m a.s.l.	age (ka)	1-σ error	MSWD	% plateau n(steps)	K/Ca	1-σ error
STR108-1		33S0518572 4295656	120	**3.9**	± 1.6 ± 39.7%	1.2	50.5 5	0.55	± 0.11
STR108-2				**4.0**	± 1.2 ± 30.2%	0.5	59.6 5	0.75	± 0.08
STR108-1+2				**4.0**	± 0.9 ± 23.4%	0.7	55.5 10	0.63	± 0.08
STR106	Piscità	33S0519673 4295584	30	**6.8**	± 1.4 ± 20.6%	0.6	97.1 7	1.14	± 0.04
STR114	Serro Adorno	33S0519307 4295876	2	**6.9**	± 1.1 ± 16.6%	0.4	95.8 8	1.24	± 0.09
STR110	Spiaggia Lunga	33S0519543 4295772	1:05	**7.7**	± 1.4 ± 18.8%	2.2	99.1 10	0.73	± 0.10
STR83 1	Nel Cannestrà	33S0519425 4294379	450	**7.0**	± 1.2 ± 15.5%	0.5	88.4 16	0.85	± 0.03
STR83 2				**9.6**	± 2.3 ± 24.4%	0.1	92.3 6	1.08	± 0.20
STR83 1+2				**7.6**	±1.1 ±14.5%	0.4	89.2 22	0.88	± 0.04
STR115b	Labronzo	33S519208 4295910	1	**8.3**	± 1.6 ± 19.4%	1.5	60.6 4	0.90	± 0.03
STR112	Dike of Labronzo	33S0519307 4295876	2	**8.2**	± 1.8 ± 21.5%	1.5	98.0 11	0.89	± 0.04
STR72b	Vallonazzo	33S0519531 4295782	2	**8.7**	± 2.0 ± 22.5%	0.7	98.4 10	1.07	± 0.08
STR65	San Vincenzo	33S0520980 4295196	1	**12.5**	± 2.6 ± 20.6%	0.7	86.4 8	1.10	± 0.12
STR117	San Bartolo	33S0519739 4295753	1	**13.1**	± 4.6 ± 40.1%	0.3	96.4 8	0.25	± 0.02
STR101	Roisa	33S0519359 4294924	275	**15.2**	±2.8 ± 18.6%	2.2	56.7 5	0.46	± 0.05
Pooled result	STR72b, 83, 106, 110 112 115b, 114, 117			**7.5**	±0.5	0.6	92.0 71	0.44	± 0.04